Langmuir

Article

pubs.acs.org/Langmuir

Toward Ion-Free Polyelectrolyte Multilayers: Cyclic Salt Annealing

Hadi M. Fares, Yara E. Ghoussoub, Richard L. Surmaitis, and Joseph B. Schlenoff*

Department of Chemistry and Biochemistry, The Florida State University, Tallahassee, Florida 32306-4390, United States

Supporting Information

ABSTRACT: Polyelectrolyte multilayers (PEMUs) are made from various combinations of polyanions and polycations. It is now understood that these ultrathin films of polyelectrolyte complex may also incorporate counterions derived from the solutions from which the PEMU was deposited or exchanged into the film postassembly. If these ions are required to compensate nonstoichiometric ratios of polycation and polyanion they cannot leave the film and exert considerable influence on film properties, such as modulus and permeability. These "extrinsic" charges also complicate fundamental studies on PEMUs. We report a method to remove almost all ionic content from a PEMU made of poly(diallyldimethylammonium chloride), PDADMAC, and poly(styrenesulfonate), PSS. In this method, a high salt concentration plasticizes the multilayer past its glass transition, dispersing all the buried excess PDADMA throughout the film. Exposure to a solution of PSS in a lower salt concentration consumes excess PDADMA near the surface without overcompensating with PSS. The process is repeated in a cyclic fashion, removing >95% of the ions charge present in the as-made PEMU.

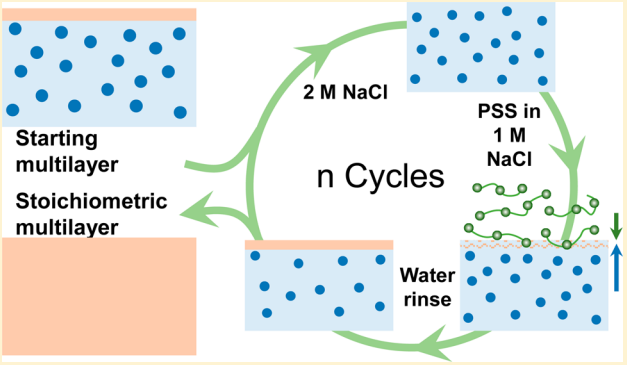

INTRODUCTION

Driven mainly by the entropic release of counterions,[1,2] polyelectrolyte multilayers, PEMUs, are made by alternating deposition of polycations and polyanions on a substrate.[3] Many potential uses of PEMUs have been reported such as functional membranes,[4−7] active and passive protective coatings,[8−10] and biomedical applications.[11−13] At first, the prevailing view of their internal stoichiometry considered the ratio of positive and negative polyelectrolyte charges to be close to 1:1,[3,14,15] although other works inferred nonstoichiometric compositions.[16−18] Balanced numbers of polymer charges would support the thesis that PEMUs contain no salt counterions (extrinsic sites, Scheme 1).[14,19] In this case, the PEMU would be seen as a tight amorphous network of polymer−polymer ion pairing interactions or intrinsic sites.

Following additional studies suggesting indirectly or showing directly the presence of counterions,[20−23] sensitive radiolabeling studies allowed us to track ion populations.[24] Counterions have emerged as key players in many of the applications at a time where fewer studies described the buildup of PEMUs[25,26] and the origin of these ions.[24,27] In addition to radiolabeling,[14,24] IR spectroscopy of IR-active counterions reveals ion content averaged over the entire PEMU[28,29] and X-ray photoelectron spectroscopy (XPS) provides elemental composition of surface counterions[30] and more insight on bulk counterions when accompanied by ion sputtering for depth profiling.[22] Other techniques such as neutron and X-ray reflectometry[16−18] have been employed to indirectly estimate ion content.

Scheme 1. Addition of PSS to a Multilayer Terminated with PDADMA Showing the Outward Diffusion of Extrinsic Positive Charge, PDADMA*, To Complex with the Incoming Polyanion at the Surface[a]

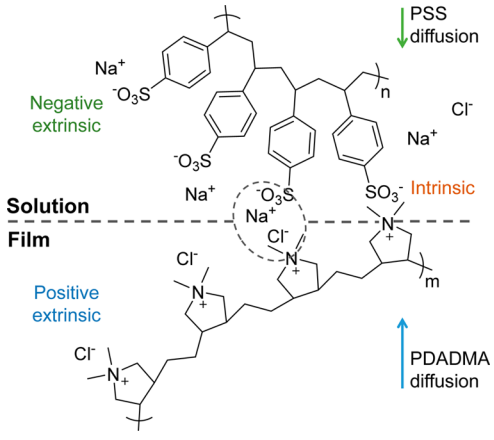

[a]The polymer/polymer ion pairing is driven by the entropic release of sodium and chloride counterions. The ladder-like pairing shown is oversimplified, and polymer−polymer contacts between different chains also occur.

Received: December 18, 2014
Revised: February 1, 2015
Published: February 22, 2015

DOI: 10.1021/la504910y
Langmuir 2015, 31, 5787−5795

Counterions were found to control many PEMU properties.[31] A higher concentration of salt—an additional source of counterions—increases the multilayer thickness.[15] The type of electrolyte, along a Hofmeister series,[32] also affects the growth of PEMUs[15,33−35] as well as their physical properties (rubbery versus glassy).[22] Because ions can be exchanged with external molecules they are important when using PEMUs as reservoirs,[36] nanocomposites,[37] membranes,[4,6] and potential systems for drug delivery.[36,38]

The ion content of a PEMU is under rapid and reversible control of the salt concentration in which the film is immersed. Thus, substantial quantities of ions may be "doped" into multilayers to control their properties. However, it is much more difficult to extract ions if they are balancing, and coupled to, nonstoichiometric polyelectrolytes. These residual ions are trapped in the PEMU, influencing all ion-related properties. Thicker multilayers, especially those exhibiting some type of nonlinear or "exponential" growth during their assembly,[25,26] may contain significant amounts of extrinsic charge. It would be useful to have a process which could be applied to a PEMU, once it has been constructed, to balance all the polymer charge, creating a truly ion free (intrinsic) film. In the present work, we describe approaches to add the polyelectrolyte needed to displace all the extrinsic charge within a PEMU. One of these techniques yielded substantial reductions of total ion content.

EXPERIMENTAL SECTION

Materials. Poly(diallyldimethylammonium chloride) (PDADMAC, molecular weight 4−5 × 10^5 g mol^{-1}), poly(4-styrenesulfonic acid) (PSS, molecular weight 7.5 × 10^4 g mol^{-1}), and sodium nitrate ($NaNO_3$, A.C.S. reagent) were used as received from Sigma-Aldrich. Sodium chloride (Fisher), conc. sulfuric acid (J. T. Baker), and hydrogen peroxide (30% solution, Macron) were also used as received. Positive radiolabeled counterions were purchased from PerkinElmer: $^{22}Na^+$ (as $^{22}NaCl$, half-life 950 days, positron, γ-emitter, E_{max} = 0.546 MeV) with a specific activity of 630 Ci g^{-1} was prepared as a stock solution of 100 μCi in 1 mL of water; ^{14}C-tetraethylammonium bromide (^{14}C TEABr, half-life 5730 years, β-emitter, E_{max} = 0.156 MeV) with a specific activity of 3.5 Ci mol^{-1} was supplied as a stock solution of 250 μCi in 2.5 mL of ethanol. The ^{125}I isotope as $Na^{125}I$, also from PerkinElmer, was used as a negative counterion: $^{125}I^-$ (half-life 60 days, γ-ray, E_{max} = 0.035 MeV), supplied as a stock solution of 1 mCi in 0.5 mL 10^{-5} M NaOH, specific activity of 17 Ci mg^{-1}. Single- and double-side polished silicon wafers were from Silicon, Inc. All solutions were prepared using deionized water (Barnstead, 18 MΩ E-pure).

Polyelectrolyte Multilayer Buildup. Silicon wafers were cleaned in a "piranha" solution (70:30 H_2SO_4:H_2O_2), rinsed thoroughly with deionized water, and dried under a stream of nitrogen. They were mounted, face down, on shafts, rotated at 300 rpm, and the buildup was carried out with a robot (StratoSequence V, NanoStrata Inc.). During the buildup, wafers were dipped sequentially in polyelectrolyte solutions. Each "layer" was made by a 5 min dipping step in polyelectrolyte solution followed by a 3 × 1 min rinsing step in consecutive water beakers. Rinse and polymer solutions were approximately 50 mL each and nominally neutral (pH ca. 6). The polyelectrolyte solutions were 10 mM with respect to the monomer units in 1.0 M NaCl. After the last rinsing step, the multilayers were dried with N_2, treated appropriately, and characterized by FTIR, scintillation counting, AFM, XPS, and streaming potential measurements. The notation $(PDADMA/PSS)_n$ refers to multilayers made of n bilayers (n = 20 is equivalent to 40 layers) of PDADMA and PSS, starting with PDADMA.

Postdeposition Treatment of PEMUs. After assembly, PEMUs were subjected to different treatments. The procedure to obtain stoichiometric multilayers is detailed here: freshly prepared PEMUs were soaked at room temperature in 2.0 M NaCl for 30 min and then in a 10 mM PSS in 1.0 M NaCl (the same solution used to prepare the multilayer) for 5 min. After each soaking step, the PEMU was washed in three consecutive water beakers for 1 min each. Each 2 M NaCl step, followed by 10 mM PSS in 1 M NaCl, with their respective water washes, constitutes one "cycle". Before any cycle (t = 0) and after each cycle the multilayer was soaked in 10^{-2} M sodium nitrate to label extrinsic positive sites, PDADMA*, triple rinsed with pure water and dried with a stream of N_2, and an FTIR spectrum was recorded. Cycles were repeated until the nitrate peak disappeared. FTIR spectra of PEMUs on double-side polished Si 100 wafers, held at 15° from perpendicular to the incident beam, were acquired using a Thermo Nicolet Avatar 360 equipped with a DTGS detector. EZ-OMNIC software was used to analyze the spectra and calculate peaks area. The background was a bare double-side polished Si wafer, and 100 scans were averaged at a resolution of 4 cm^{-1}. The nitrate peak area was measured between 1290 and 1400 cm^{-1}. Nitrate soaking time was decided after monitoring the peak area with different soaking times: after 5 min the peak area remained constant.

Dry thickness of thin PEMUs (20 layers) was acquired with a Gaertner Scientific L116B Autogain ellipsometer with 632.8 nm radiation. The incident angle was fixed at 70°, and the refractive index was set to 1.55. Images of dry PEMUs were acquired with a MFP-3D AFM (Asylum Research Inc., Santa Barbara, CA) equipped with an ARC2 controller and silicon NCHV probes (Veeco, radius = 10 nm, spring constant 20−80 N m^{-1}). The ac mode was used to monitor morphological changes, thickness, and roughness of PEMUs. The cantilever was tuned to 10% below its resonance frequency. A scan size of 20 μm^2 was used to obtain the roughness: the roughness of 10 1 × 1 μm areas were averaged. To obtain the thickness of $(PDADMA/PSS)_{15\text{ and }20}$, a scratch was made across the PEMU and the step height of the film was measured. Three or four thickness measurements were averaged. For images showing morphology, a scan size of 5 μm^2 was used.

Radiolabeling and Radiocounting Measurements. Like the FTIR experiment using NO_3^-, radiolabeling was used as an ion exchange-based technique to quantify the ions within the PEMU. $^{22}Na^+$ was used for the total negative sites and ^{14}C-TEA$^+$ for the surface sites. The latter does not penetrate the PEMU when it is capped with PSS.[24] To label positive extrinsic sites, $^{125}I^-$ was used. Except for the TEA$^+$, the specific activity of the radiolabeled solutions was set by diluting the "hot" (radiolabeled) solution with "cold" (unlabeled) solution. The specific activity determines the precision and accuracy of the counting, and the concentration ensures a large excess of radiolabel in solution. A concentration of 1.0 × 10^{-4} M $^{22}NaCl$ at 5 Ci mol^{-1} was prepared by mixing 254.6 μL of the "hot" stock solution and 49.8 mL of unlabeled 1.0 × 10^{-4} M NaCl. To prepare a 2 Ci mol^{-1} solution of 1.0 × 10^{-3} M $Na^{125}I$, 126 μL of the labeled solution was added to 99.9 mL of "cold" 1.0 × 10^{-3} M NaI. ^{14}C TEABr, 1.0 × 10^{-4} M, was prepared by mixing 175 μL of the stock solution with 49.8 mL of water to obtain a specific activity of 3.5 Ci mol^{-1}.

For radiocounting, 3 mm thick plastic scintillator sheets (SCSN-81, Kuraray America) were cut into 1.5 in. diameter disks and placed on the 2 in. window of a photomultiplier tube (PMT, RCA 8850) on top of a drop of immersion oil to ensure good optical contact. The PMT, in a dark box, was connected to a Bertan 313B high-voltage supply generating 2300 V. Counts were recorded by a frequency counter (Philips PM6654C) interfaced with a computer running LabView software. The gate time was 10 s, and the pulse threshold was −20 mV. The counting efficiency (i.e,. the number of counts per second divided by the disintegrations per second) was about 14% for iodine, 46% for TEA, and more than 90% for sodium. The total number of counts for each data point ranged from 11 000 to 4 300 000 with respective counting errors from ±1% to ±0.05%.

After treating the PEMUs, they were washed, dried, and immersed in about 5 mL of the radiolabeled solutions for 15 min for TEA$^+$ and 30 min for $^{22}Na^+$ and $^{125}I^-$. Wafers were then removed from the solutions and dried, without rinsing, with a strong stream of N_2. They were then placed, face down, on the plastic scintillator and counted for 15 min. After counting, they were rinsed with water and placed in an

DOI: 10.1021/la504910y
Langmuir 2015, 31, 5787−5795

unlabeled solution of 10^{-2} M $NaNO_3$ to exchange out all the radiolabel. This step lasted for 5−30 min depending on the amount of extrinsic sites found in the multilayer. Calibration curves were created by dispensing 1−5 μL aliquots of the "hot" solution on top of the scintillator and covering it with a bare Si wafer to ensure good spreading. The curve (counts versus number of moles) was used to convert counts to number of moles and then divided by area to give mol m^{-2}.

X-ray Photoelectron Spectroscopy. XPS was performed using a PerkinElmer (PHI 5100 series) with a base pressure of 1.9×10^{-8} Torr. A noncollimated Mg Kα X-ray source ($h\nu$ = 1253.6 eV) was used to produce photoelectrons, and spectra were acquired at a takeoff angle of 45° averaging 20 scans at a speed of 0.1 eV s^{-1}.

Zeta Potentials. Streaming potentials were measured using a spinning disk method introduced by Sides et al.[39,40] and recently validated for PDADMA/PSS multilayers.[41] Briefly, multilayers were built on a 1 in. diameter fused silica disk which was press fit on the end of a dc motor (Portescap). At 1 mm from the center of the disk, an AgCl-coated silver wire was placed acting as one electrode while another silver electrode was placed close to the side of a 250 mL cell fitted with a water jacket and maintained at 20 °C. A dc power supply (BK precision Multi Range 60 V/5 A) powered the motor, while three aluminum baffles minimized vortexing. Using an electrometer (Keithley 617) interfaced to a computer running Labview software, the streaming potential was measured between Ag electrodes in a 10^{-4} M NaCl solution before and after the two steps of one full annealing/PSS cycle for an as-made $(PDADMA/PSS)_{15}$ multilayer. The streaming potential, Φ_s, was converted to the zeta potential, ζ, using the following equation[39,41]

$$\zeta = \frac{1.96\kappa\nu^{1/2}}{\varepsilon a \Omega^{3/2}} \frac{1}{2\left(1 - \frac{z}{a} - \frac{1}{2\left(\frac{z^2}{a^2}+1\right)^{1/2}}\right)} \Phi_s \quad (1)$$

where a, Ω, ν, κ, and z are the disk radius (m), disk rotation rate (s^{-1}), kinematic viscosity (m^2 s^{-1}), solution conductivity, and axial distance from the disk (m), respectively. ε is the permittivity of water at 20 °C ($\varepsilon = \varepsilon_r\varepsilon_0$, with ε_r being the relative permittivity (80.5 at 20 °C) and ε_0 the vacuum permittivity (8.85×10^{-12} F m^{-1})). All data were from the *CRC Handbook of Chemistry and Physics*.[42] The rotation rate was typically 2585 rpm.

RESULTS AND DISCUSSION

Obtaining a fully intrinsic PEMU can be a challenge. $(PDADMA/PSS)_n$ multilayers thicker than about 12 layers have been shown to contain a large amount of PDADMA* compensated by chloride counterions.[24] Under "linear" assembly conditions (about 1.0 M NaCl and below) these PEMUs contain very little sodium, indicating a corresponding low population of negative extrinsic sites (PSS*).[24] According to our recent model, the excess PDADMA* resides throughout the film when PDADMA is the "top" or last-added layer and under a skin of intrinsic (stoichiometric) polyelectrolyte complex when PSS is the top layer.[24] The persistent excess of PDADMA*, revealed with $^{125}I^-$ (radioactive) or NO_3^- (IR active), affects many properties of the PEMU, including mechanical properties[43] and ion permeability.[24] As a consequence of the latter, PSS/PDADMA multilayers do not exclude negative ions as well as they would were they completely intrinsic.[24]

Extrinsic charge is an inevitable result of kinetic limitations in the multilayering process itself. Multiple interactions between polyelectrolyte chains with other chains slow down the interdiffusion of polyelectrolyte molecules by many orders of magnitude compared to diffusion in dilute or even semidilute solutions.[44] Incoming polyelectrolyte complexes with oppositely charged repeat units near the surface as shown in Scheme 1. In this reaction−diffusion model the motion of the complex stops on the time scale of the multilayering after the addition of a fixed amount of polymer,[45] so each PSS or PDADMA layer adds the same amount, and the PEMU grows "linearly".

In the kinetics of multilayering a rapid initial quantity of material adsorbs followed by a much slower addition.[46] For experimental purposes, a limited time must be selected (usually 5−20 min) for each dip in order to make a multilayer in a reasonable time. More polymer can always be added with more time.[15] On one hand, kinetic limitations may slow multilayer growth to unacceptable rates; on the other hand, the limitations are responsible for the fuzzy layering[3] of some components (i.e. actual "multilayering.")

Nonequilibrium assembly leads to inhomogeneous compositions in PEMUs. As an example, when PDADMA* in $(PDADMA/PSS)_{20}$, built here in 1 M NaCl, is labeled with $^{125}I^-$ it is seen that about one-third of the total amount of polycation PDADMA exists as PDADMA* (i.e., one-third of the polymer charge is extrinsic). One possible approach to eliminating this significant nonstoichiometry could be to simply allow the "slower" component, here PSS, enough time to find all available PDADMA* extrinsic sites. An example of this strategy is shown in Figure 1, where as-built $(PDADMA/PSS)_{20}$ was subjected to additional 5 min immersions in the same PSS used for buildup. The amount of PDADMA* was assessed by exchanging Cl^- ion in PDADMA(Cl) with NO_3^- and detecting the PDADMA(NO_3) with FTIR. Some additional PSS entered the film to pair with PDADMA*, as seen in Figure 1, which also depicts the convenient spectral regions used for PDADMA, NO_3^-, and PSS quantification (the

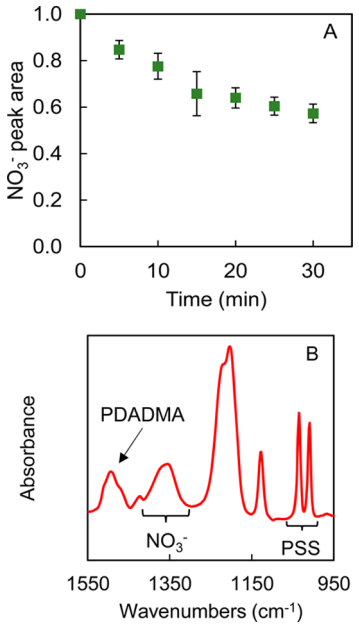

Figure 1. (A) Positive bulk extrinsic sites (PDADMA*), normalized to the as-made PEMU, in $(PDADMA/PSS)_{20}$. Extrinsic sites are estimated by the nitrate peak area in FTIR following exposure to 10 mM PSS in 1 M NaCl. PEMU is labeled with NO_3^- ion (in a solution of 10^{-2} M $NaNO_3$) by ion exchange with Cl^-. Loss of NO_3^- is due to PSS adding to the film. Error bars are +/− 1 std. dev. (B) Nitrate, PDADMA, and PSS peaks integrated to estimate the amounts of polymers and positive extrinsic sites.

DOI: 10.1021/la504910y
Langmuir 2015, 31, 5787−5795

PDADMA band contains a 5% contribution from PSS which was subtracted for quantitative studies).

Additional detail of the FTIR experiments, showing that the PDADMA band remained constant (no loss of PDADMA) and the PSS band increased slowly, confirms a partial approach toward stoichiometry (Figure S1, Supporting Information). When the time of immersion in PSS (1 M NaCl) was substantially increased, to 8 h, the nitrate peak area disappeared (Figure S2, Supporting Information). Labeling the PDADMA* with $^{125}I^-$ (Figure S3, Supporting Information) echoed the FTIR results using NO_3, but the $^{22}Na^+$ probe revealed a significant increase in the amount of PSS*, i.e., the amount of PSS "overshoots" the amount needed to compensate PDADMA*. It may be that 5 min of immersion in PSS solution is not enough time to allow for overcompensation by PSS.

To accelerate the rate of access of PSS to PDADMA* within a film we exploited a recent finding that the PSS/PDADMA complex undergoes a room-temperature glass transition for [NaCl] > 1.5 M, enhancing the interdiffusion rate,[47,48] which allows more PSS to enter the film faster.[49] Nascent $(PDADMA/PSS)_{20}$ was immersed in 10 mM PSS containing 2 M NaCl for increasing intervals of time. Figure 2 shows

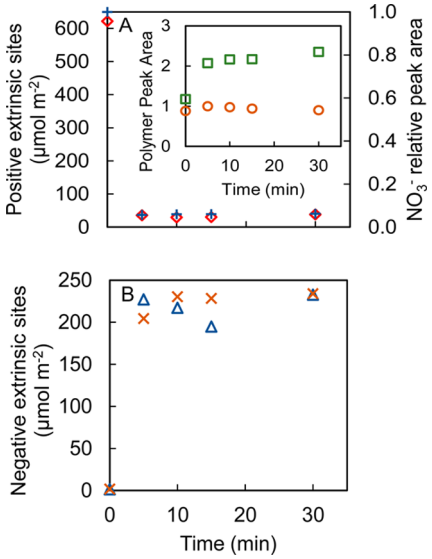

Figure 2. (A) Positive extrinsic sites detected by radiolabeling with ^{125}I (◇) and nitrate labeling with FTIR (+) in a $(PDADMA/PSS)_{20}$ during addition of 10 mM PSS in 2 M NaCl. (Inset) PDADMA (○) and PSS (□) FTIR peak area during the same addition. (B) Negative extrinsic sites radiolabeled by ^{22}Na (△) and surface negative extrinsic sites (×) radiolabeled by ^{14}C TEA^+ in the same sample during the same experiment.

apparent success with elimination of PDADMA* with the first 5 min immersion in this solution. Unfortunately, $^{22}Na^+$ shows the PEMU now contains a large amount of excess PSS* (Figure 2). ^{14}C-TEA is now able to access all PSS*, giving similar results to $^{22}Na^+$ (Figure 2). In addition, control experiments with soaking in 2 M NaCl (i.e., no PSS, Supporting Information Figure S4) reveal the loss of PDADMA. This is an example of salt "etching" of PEMUs recently explored for the PSS/PDADMA system.[50] Removal of excess PDADMA by etching is one way to approach stoichiometry, but it was found to be slow and incomplete (Figure S5, Supporting Information) even after 160 h. PDADMA is lost at a faster rate than PSS, in agreement with the results of Han et al. (Figure S5, Supporting Information).[50] Because 2 M NaCl is not sufficient to dissolve the PEMU the polyelectrolytes probably leave the film as polyelectrolyte complex nanoparticles, stabilized by a shell of excess PDADMA.[51]

A treatment was devised to take advantage of chain mobilization induced by 2 M NaCl and compensation without overcompensation that occurred in 1 M NaCl. This treatment is summarized in Scheme 2. The as-made PEMU was first

Scheme 2. Proposed Mechanism of the Cycling Technique (2 M NaCl/10 mM PSS in 1 M NaCl) Used To Turn (PDADMA/PSS) PEMU into an Intrinsic Multilayer: (A) Starting Multilayer; (B) Final Intrinsic Multilayer[a]

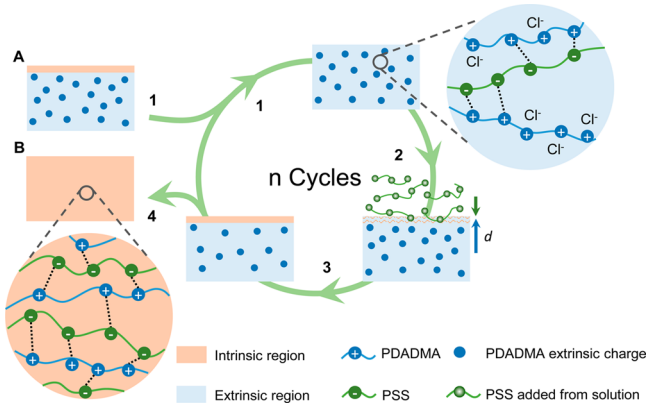

[a](1) 2 M NaCl for 30 min. (2) 10 mM PSS in 1 M NaCl for 5 min. (3) Water rinse. (4) Result after all cycles are done.

immersed briefly in 2 M NaCl (containing no PSS) to promote dispersion of PDADMA* throughout the film (step 1); the film was then immersed in 10 mM PSS in 1 M NaCl (step 2), which allows the PDADMA* near the surface to react with incoming PSS from solution (step 3). This step leaves a PEMU with a skin of intrinsic charge and a buried layer of extrinsic charge, as before, but the PDADMA* concentration is lower. Steps 1, 2, and 3 were repeated (Scheme 2) in a cyclic manner until almost all the PDADMA* could be coaxed from the PEMU.

Figure 3 illustrates that this cyclic salt annealing procedure works well. Figure 3A shows the drop in PDADMA* for each cycle, approaching zero after the 7th cycle. At the same time, the population of PSS* does not increase much (Figure 3A). The PSS* results are expanded in Figure 3B to show less than 1% of the PSS is PSS*. Probing PDADMA* with $^{125}I^-$ gives results similar to the FTIR method but has a more sensitive detection limit, revealing 1.2% PDADMA* after 7 cycles (Figure S6, Supporting Information). The concentration of surface PSS* also increases, approaching a monolayer (ca. 2.5×10^{-6} moles m^{-2}). FTIR spectra (Figure 4) showed no discernible change in the amount of PDADMA while the amount of PSS in the film increased, as expected.

The choice of 2 M NaCl for step 1 is justified by Figure S7, Supporting Information, which shows that a salt concentration of 2 M is more effective than lower concentrations (a range between 0.75 and 1.75 M) at reducing the original amount of PDADMA* after 6 cycles. The 30 min duration of this same step yielded better results than 10 and 20 min (Figure S8, Supporting Information).

Analysis by XPS supplied more information on the surface composition (to a depth of 8 nm) during a cycle (see Figure S9,

DOI: 10.1021/la504910y
Langmuir 2015, 31, 5787−5795

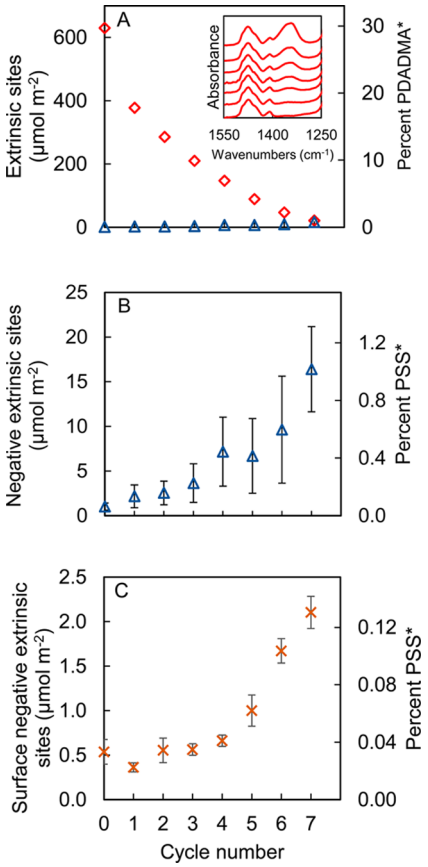

Figure 3. (A) Total positive extrinsic sites and percent of the total amount of PDADMA that is PDADMA* (◇). (B) Total negative extrinsic sites and percent of the total PSS that is PSS* (△). (C) Negative extrinsic sites at the surface and percent of total PSS these sites represent (×). Sites are radiolabeled by ^{125}I, ^{22}Na, and ^{14}C TEA^+ in $(PDADMA/PSS)_{20}$ during cycles of 2 M NaCl/10 mM PSS in 1 M NaCl. (Inset in A) FTIR spectra depicting PDADMA (left) and NO_3^- (right) peak during the cycles.

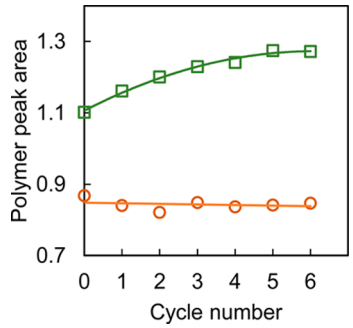

Figure 4. PSS (990–1095 cm^{-1}) (□) and PDADMA (1427–1525 cm^{-1}) (○) FTIR peak areas obtained during cycling of a multilayer in 2 M NaCl for 30 min and then 10 mM PSS in 1 M NaCl for 5 min (both steps constituting 1 cycle). Lines are a guide to the eye.

Supporting Information, for raw XPS scans). The starting $(PDADMA/PSS)_{15}$ had a nitrogen to sulfur ratio (N/S) close to 1:1 (see Figure 5A) with a slightly larger amount of S since the last layer was PSS. Soaking it in 2 M NaCl for 30 min showed more PDADMA at the surface, now giving a N/S of about 1.4:1. The last step in the cycle returned the multilayer surface to its original N/S composition of ca. 1:1. The increase

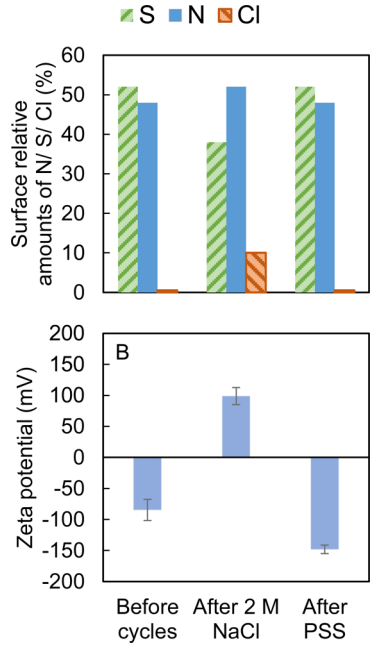

Figure 5. (A) Amounts of sulfur (PSS), nitrogen (PDADMA), and chloride (PDADMA*) at the surface of $(PDADMA/PSS)_{15}$ obtained by XPS during the first cycle of 2 M NaCl and then 10 mM PSS in 1 M NaCl. Element compositions are relative, given as atomic % with %N + %S + %Cl = 100. (B) Surface zeta potential of $(PDADMA/PSS)_{15}$ obtained from the streaming potentials measured by the spinning disk method during the first cycle (2 M NaCl followed by 10 mM PSS in 1 M NaCl). [NaCl] is 10^{-4} M, the electrode distance is 1 mm, and the spinning rate is 2585 rpm.

in Cl content tracks the additional PDADMA* brought to the surface.

Assuming the density of the PEMU to be 1.1 g cm^{-3}, using the radiolabeling data of the 570 nm thick $(PDADMA/PSS)_{20}$ in Figure 3A, about 30% of the total PDADMA is PDADMA* in the 40-layer film. A 1.4:1 ratio of N:S after annealing in Figure 5 means the 29% of the surface PDADMA is PDADMA* (i.e., 71% is paired with PSS). Therefore, following a 2 M NaCl annealing step, the concentration of PDADMA* is the same inside the multilayer and on the surface of the PEMU. This suggests that 2 M NaCl does, indeed, disperse the PDADMA* extrinsic sites uniformly throughout the PEMU as Scheme 2 depicts.

The zeta potential tracked the anticipated switch in charge on one full cycle. The spinning disk generates a streaming potential that is not compromised by surface conductivity.[52] This potential was measured using two silver indicator electrodes—one placed near the disk on its axis and one in the bulk solution.[53] The streaming potential was the difference in measured potential between the disk *on* and *off*. Examples of the raw data are provided in Figure S10, Supporting Information. In agreement with our previous results[41] the starting zeta potential of a PSS-capped PEMU was around −85 mV (Figure 5B). When the PEMU was annealed in 2 M NaCl, the potential switches to around +100 mV, demonstrating charge reversal as PDADMA* migrates to and appears at the surface. The zeta potential then switches back to a negative value (−150 mV) with the addition of PSS, showing excess PSS* at the surface. The reason the surface potential of the cycled PEMU is more negative than that of the starting multilayer is not known.

DOI: 10.1021/la504910y
Langmuir 2015, 31, 5787–5795

Mechanism. Since the beginnings of the modern era of investigations into such systems it has been recognized that overcompensation of surface charge by incoming polyelectrolyte is essential for multilayer propagation.[3,54] The discovery of strongly nonlinear, or "exponential", growth[25,55] emphasized enhanced mobility of at least one polymeric component in some systems/conditions.[56] However, nonlinear growth of the beginning few layers is observed in almost all multilayers, even those considered to be growing "linearly" (constant thickness increment versus layer number). Using a combination of nanoindentation,[57] XPS, imaging, and radiochemistry[24] we reported that surface overcompensation in PSS/PDADMA grown in "linear" conditions (<1 M) occurred only following the addition of the positive polymer. The PSS "layer" gave near-zero (intrinsic) surface charge.

In the mechanism for (asymmetric) multilayering the excess PDADMA (i.e., PDADMA*) produced by overcompensation meets and complexes with incoming solution PSS in a region near the PEMU surface as in Scheme 1.[24] In this reaction–diffusion zone the mobility of polymers decreases until, when the zone is intrinsic and glassy, polymers stop moving. Thus, the addition of the PSS layer is limited by the amount of material it takes to form this glassy zone. For reasons not yet understood, the reaction–diffusion length of PDADMA* in PSS/PDADMA complex is longer than that of PSS*, but it is finite, so not all the PDADMA* in the multilayer is used up. A buried layer of PDADMA* thus grows. The finding that the PSS layer thickness depends inversely on PSS molecular weight supports this model.[48] Only multilayers which grow on the order of one monolayer (<1 nm) per cycle can be expected to approach linearity for all layers, with minimized asymmetry and close to 1:1 stoichiometry. Of course, all reaction/diffusion "lengths" depend on the time scale of the experiment. Even with this kinetic limitation, sufficient time allows all PDADMA* to complex with PSS (Figure S2, Supporting Information) but PSS ultimately overcompensates.

Such a model is implied in Scheme 2 and illustrated more clearly in Figure 6, which depicts starting multilayers of different thicknesses. Each exposure to 2 M NaCl mobilizes and disperses evenly all the PDADMA* in the PEMU. On each 5 min exposure to PSS in 1 M NaCl, PDADMA* diffuses out[56] to meet PSS in the reaction/diffusion zone, which is estimated to be on the order of 70 nm thick. The PDADMA* is supplied from the bulk of the PEMU down to a depth, d. In the simplest model this supply depth is assumed to remain independent of the thickness, T, of the starting PEMU and also independent of the concentration of PDADMA*. T increases less than 10% for the entire annealing and is assumed to remain constant. If N_x is the percentage of the original (N_0 = 100%) PDADMA* remaining after x cycles

$$N_x = N_o - \left[\sum_{x=1}^{n} \frac{d}{T}(N_{x-1})\right] \quad (2)$$

The experimental results for starting PEMUs of different thicknesses are shown in Figure 6 together with the fit to eq 2 using d = 230 nm. The fits are reasonable given the simplicity of the model. d probably also depends on the total [PDADMA*].

According to salt-temperature equivalence for polyelectrolyte complexes[47] an increase in temperature should promote the same mobility as an increase in salt concentration. For the present PDADMA/PSS system, a change from 1 to 2 M NaCl is about equivalent to an increase in temperature to 45 °C.[47]

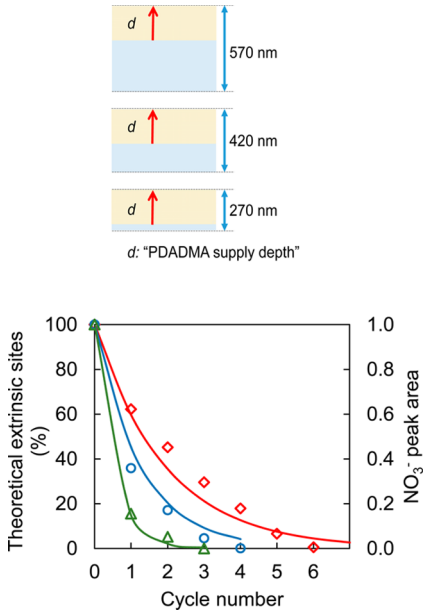

Figure 6. (Top) Scheme showing the depth from which PDADMA* is supplied during formation of the PSS "layer" in 1 M NaCl in 40-, 30-, and 20-layer PEMUs. (Bottom) Amount of PDADMA* measured with FTIR using the NO_3^- probe and the amount predicted by the model (lines) for the cycling of 20- (□), 30- (○), and 40-layer (◇) PDADMA/PSS between 2 M NaCl and 10 mM PSS in 1 M NaCl. PDADMA* supply depth, d, is 230 nm.

Thus, $(PDADMA/PSS)_{20}$ was immersed in 1 M NaCl at 45 °C for the annealing steps and then in 10 mM PSS in 1 M NaCl at room temperature as with the cyclic salt annealing. The elimination of PDADMA* was faster, needing only 2 cycles

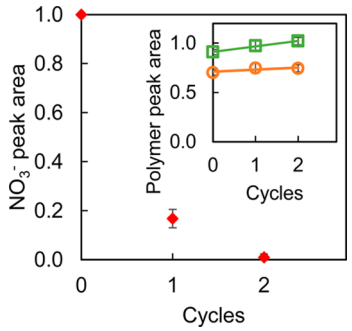

Figure 7. Positive extrinsic sites in $(PDADMA/PSS)_{20}$ during cycles of 1 M at 45 °C/10 mM PSS in 1 M NaCl at room temperature. (Inset) PSS (990–1095 cm^{-1}) (□) and PDADMA (1427–1525 cm^{-1}) (○) FTIR peak areas during the same cycles. Lines are a guide to the eye.

(Figure 7), compared to salt annealing. Radiolabeling with $^{22}Na^+$ showed about 1% of PSS was in the PSS* form. Figure S11 (Supporting Information) shows a comparison of the amounts of sodium left in the PEMU after four different techniques used to decrease PDADMA*. Though thermal annealing appears faster, AFM revealed a rougher surface for the thermally cycled PEMU than that for salt cycled (Figure 8). This difference in roughness may be due to the faster immobilization of polymers in PEMUs going from hot to cold water than from higher to lower salt, the latter allowing more time for relaxation. Furthermore, the number of cycles needed for thermal cycling was less consistent than for salt

DOI: 10.1021/la504910y
Langmuir 2015, 31, 5787–5795

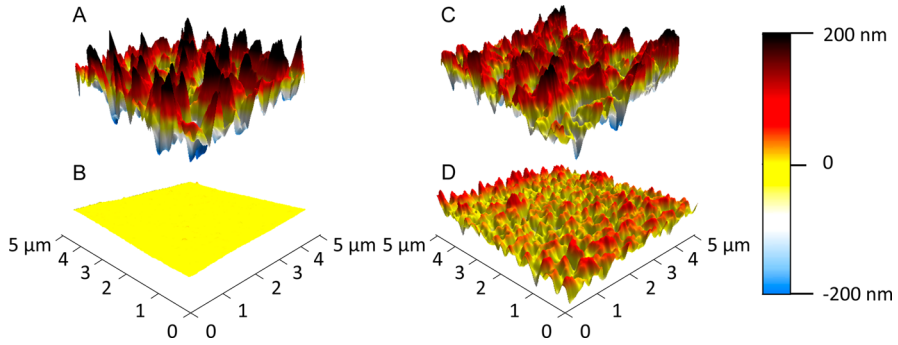

Figure 8. AFM images of (A) $(PDADMA/PSS)_{20}$ built in 1 M NaCl and (B) the same PEMU after 7 cycles of 2 M NaCl/10 mM PSS in 1 M NaCl. Respective rms roughnesses 79 and 5 nm. AFM images of (C) $(PDADMA/PSS)_{20}$ built in 1 M NaCl and (D) the same PEMU after 2 cycles of 1 M at 45 °C/10 mM PSS in 1 M NaCl with respective rms roughnesses of 65 and 20 nm.

cycling for reasons not immediately apparent. Temperature-salt equivalence may not hold for polyelectrolyte complexes with extrinsic charge.

Of the strategies to convert as-made PEMUs from extrinsic to intrinsic it was found that cycling in 2 M NaCl and then in 10 mM PSS in 1 M NaCl was the most consistently effective, leading to minimal PDADMA* and PSS*. All fuzzy layering within the PEMU is erased,[45] giving a thin, stoichiometric film of polyelectrolyte complex. Such a morphology makes interpretation and prediction of properties more straightforward. An additional benefit of cyclic salt annealing is shown in the AFM images in Figure 8A and 8B. Prior to cycling $(PDADMA/PSS)_{20}$ has significant roughness (79 nm), as seen previously.[48] After cyclic annealing the surface roughness decreases substantially (here to 5 nm)—less than 1% of the film thickness. Annealing in salt causes smoothing of the surface via interdiffusion.[58] The roughness is less than that (15 nm) seen for an annealed 500 nm PDADMA/PSS film[48] because extrinsic sites have been removed, minimizing water content, maximizing modulus, and reducing the dimensional changes of the film on swelling and drying. These dimensional changes, constrained to the direction perpendicular to the substrate, cause stresses and buckling within the film.[59,60]

CONCLUSIONS

The term "polyelectrolyte multilayers" describes better how these ultrathin films of polyelectrolyte complex are made rather than their actual morphology. Any layering within the film is diffuse and requires careful design to build in.[3] In most applications, multilayers are presumed to be rather uniform, an assumption that may not hold. Here, uniformity of composition has been induced by alternating between two salt concentrations: 2 M NaCl to "scramble" the residual excess polymer (PDADMA*) and 1 M NaCl with PSS to consume the PDADMA* that lies within a certain supply depth within the film. This cyclic treatment leaves the film almost fully ion free (intrinsic) and far smoother than the as-made multilayer. Salt conditions needed for annealing will depend on the polyelectrolytes and the salt employed. For example, polyelectrolyte pairs such as PAH/PSS which associate more strongly will require a high concentration of NaCl for annealing or the use of a more disruptive salt along the Hofmeister series, such as NaSCN.

ASSOCIATED CONTENT

Supporting Information

Extrinsic site concentration versus time for various controls; raw XPS and streaming potential data. This material is available free of charge via the Internet at http://pubs.acs.org.

AUTHOR INFORMATION

Corresponding Author

*E-mail: schlen@chem.fsu.edu.

Notes

The authors declare no competing financial interest.

ACKNOWLEDGMENTS

We thank Dr. Qifeng Wang for valuable discussion. This work was supported by the National Science Foundation (grant DMR-1207188).

REFERENCES

(1) Michaels, A. S. Polyelectrolyte Complexes. *J. Ind. Eng. Chem.* **1965**, *57*, 32−40.
(2) Bucur, C. B.; Sui, Z.; Schlenoff, J. B. Ideal Mixing in Polyelectrolyte Complexes and Multilayers: Entropy Driven Assembly. *J. Am. Chem. Soc.* **2006**, *128*, 13690−13691.
(3) Decher, G. Fuzzy Nanoassemblies: Toward Layered Polymeric Multicomposites. *Science* **1997**, *277*, 1232−1237.
(4) Krasemann, L.; Tieke, B. Selective Ion Transport Across Self-assembled Alternating Multilayers of Cationic and Anionic Polyelectrolytes. *Langmuir* **2000**, *16*, 287−290.
(5) Stroeve, P.; Vasquez, V.; Coelho, M. A. N.; Rabolt, J. F. Gas Transfer in Supported Films Made by Molecular Self-assembly of Ionic Polymers. *Thin Solid Films* **1996**, *284−285*, 708−712.
(6) Dai, J. H.; Balachandra, A. M.; Lee, J. I.; Bruening, M. L. Controlling Ion Transport through Multilayer Polyelectrolyte Membranes by Derivatization with Photolabile Functional Groups. *Macromolecules* **2002**, *35*, 3164−3170.
(7) Harris, J. J.; Stair, J. L.; Bruening, M. L. Layered Polyelectrolyte Films as Selective, Ultrathin Barriers for Anion Transport. *Chem. Mater.* **2000**, *12*, 1941−1946.
(8) Dai, J.; Sullivan, D. M.; Bruening, M. L. Ultrathin, Layered Polyamide and Polyimide Coatings on Aluminum. *Ind. Eng. Chem. Res.* **2000**, *39*, 3528−3535.
(9) Etienne, O.; Gasnier, C.; Taddei, C.; Voegel, J. C.; Aunis, D.; Schaaf, P.; Metz-Boutigue, M. H.; Bolcato-Bellemin, A. L.; Egles, C. Antifungal Coating by Biofunctionalized Polyelectrolyte Multilayered Films. *Biomaterials* **2005**, *26*, 6704−6712.
(10) Andreeva, D. V.; Fix, D.; Möhwald, H.; Shchukin, D. G. Buffering Polyelectrolyte Multilayers for Active Corrosion Protection. *J. Mater. Chem.* **2008**, *18*, 1738−1740.

DOI: 10.1021/la504910y
Langmuir 2015, 31, 5787−5795

(11) Ai, H.; Jones, S.; Lvov, Y. Biomedical Applications of Electrostatic Layer-by-layer Nano-assembly of Polymers, Enzymes, and Nanoparticles. *Cell Biochem. Biophys.* **2003**, *39*, 23−43.
(12) Boudou, T.; Crouzier, T.; Ren, K.; Blin, G.; Picart, C. Multiple Functionalities of Polyelectrolyte Multilayer Films: New Biomedical Applications. *Adv. Mater.* **2010**, *22*, 441−67.
(13) Yang, S. Y.; Mendelsohn, J. D.; Rubner, M. F. New Class of Ultrathin, Highly cell-adhesion-resistant Polyelectrolyte Multilayers with Micropatterning Capabilities. *Biomacromolecules* **2003**, *4*, 987−994.
(14) Schlenoff, J. B.; Ly, H.; Li, M. Charge and Mass Balance in Polyelectrolyte Multilayers. *J. Am. Chem. Soc.* **1998**, *120*, 7626−7634.
(15) Dubas, S. T.; Schlenoff, J. B. Factors Controlling the Growth of Polyelectrolyte Multilayers. *Macromolecules* **1999**, *32*, 8153−8160.
(16) Schmitt, J.; Grunewald, T.; Decher, G.; Pershan, P. S.; Kjaer, K.; Lösche, M. Internal Structure of Layer-by-Layer Adsorbed Polyelectrolyte Films - a Neutron and X-Ray Reflectivity Study. *Macromolecules* **1993**, *26*, 7058−7063.
(17) Hoogeveen, N. G.; Stuart, M. A. C.; Fleer, G. J.; Bohmer, M. R. Formation and Stability of Multilayers of Polyelectrolytes. *Langmuir* **1996**, *12*, 3675−3681.
(18) Lösche, M.; Schmitt, J.; Decher, G.; Bouwman, W. G.; Kjaer, K. Detailed Structure of Molecularly Thin Polyelectrolyte Multilayer Films on Solid Substrates as Revealed by Neutron Reflectometry. *Macromolecules* **1998**, *31*, 8893−8906.
(19) Schönhoff, M. Self-assembled Polyelectrolyte Multilayers. *Curr. Opin. Colloid Interface Sci.* **2003**, *8*, 86−95.
(20) Klitzing, R. v.; Wong, J. E.; Jaeger, W.; Steitz, R. Short Range Interactions in Polyelectrolyte Multilayers. *Curr. Opin. Colloid Interface Sci.* **2004**, *9*, 158−162.
(21) Caruso, F.; Lichtenfeld, H.; Donath, E.; Möhwald, H. Investigation of Electrostatic Interactions in Polyelectrolyte Multilayer Films: Binding of Anionic Fluorescent Probes to Layers Assembled onto Colloids. *Macromolecules* **1999**, *32*, 2317−2328.
(22) Salomäki, M.; Laiho, T.; Kankare, J. Counteranion-controlled Properties of Polyelectrolyte Multilayers. *Macromolecules* **2004**, *37*, 9585−9590.
(23) Farhat, T. R.; Schlenoff, J. B. Doping-controlled Ion Diffusion in Polyelectrolyte Multilayers: Mass Transport in Reluctant Exchangers. *J. Am. Chem. Soc.* **2003**, *125*, 4627−4636.
(24) Ghostine, R. A.; Markarian, M. Z.; Schlenoff, J. B. Asymmetric Growth in Polyelectrolyte Multilayers. *J. Am. Chem. Soc.* **2013**, *135*, 7636−7646.
(25) Picart, C.; Lavalle, P.; Hubert, P.; Cuisinier, F. J. G.; Decher, G.; Schaaf, P.; Voegel, J. C. Buildup Mechanism for Poly(L-lysine)/hyaluronic Acid Films onto a Solid Surface. *Langmuir* **2001**, *17*, 7414−7424.
(26) Picart, C.; Mutterer, J.; Richert, L.; Luo, Y.; Prestwich, G. D.; Schaaf, P.; Voegel, J. C.; Lavalle, P. Molecular Basis for the Explanation of the Exponential Growth of Polyelectrolyte Multilayers. *Proc. Natl. Acad. Sci. U.S.A.* **2002**, *99*, 12531−12535.
(27) Crouzier, T.; Picart, C. Ion Pairing and Hydration in Polyelectrolyte Multilayer Films Containing Polysaccharides. *Biomacromolecules* **2009**, *10*, 433−442.
(28) Farhat, T. R.; Schlenoff, J. B. Ion Transport and Equilibria in Polyelectrolyte Multilayers. *Langmuir* **2001**, *17*, 1184−1192.
(29) Schlenoff, J. B.; Rmaile, A. H.; Bucur, C. B. Hydration Contributions to Association in Polyelectrolyte Multilayers and Complexes: Visualizing Hydrophobicity. *J. Am. Chem. Soc.* **2008**, *130*, 13589−13597.
(30) Sukhorukov, G. B.; Schmitt, J.; Decher, G. Reversible Swelling of Polyanion/polycation Multilayer Films in Solutions of Different Ionic Strength. *Ber. Bunsen-Ges. Phys. Chem.* **1996**, *100*, 948−953.
(31) Klitzing, R. v. Internal Structure of Polyelectrolyte Multilayer Assemblies. *Phys. Chem. Chem. Phys.* **2006**, *8*, 5012−5033.
(32) Salomäki, M.; Tervasmäki, P.; Areva, S.; Kankare, J. The Hofmeister Anion Effect and the Growth of Polyelectrolyte Multilayers. *Langmuir* **2004**, *20*, 3679−3683.
(33) Mermut, O.; Barrett, C. J. Effects of Charge Density and Counterions on the Assembly of Polyelectrolyte Multilayers. *J. Phys. Chem. B* **2003**, *107*, 2525−2530.
(34) Wong, J. E.; Zastrow, H.; Jaeger, W.; von Klitzing, R. Specific Ion versus Electrostatic Effects on the Construction of Polyelectrolyte Multilayers. *Langmuir* **2009**, *25*, 14061−14070.
(35) Buscher, K.; Graf, K.; Ahrens, H.; Helm, C. A. Influence of Adsorption Conditions on the Structure of Polyelectrolyte Multilayers. *Langmuir* **2002**, *18*, 3585−3591.
(36) Chung, A. J.; Rubner, M. F. Methods of Loading and Releasing Low Molecular Weight Cationic Molecules in Weak Polyelectrolyte Multilayer Films. *Langmuir* **2002**, *18*, 1176−1183.
(37) Zan, X. J.; Su, Z. H. Incorporation of Nanoparticles into Polyelectrolyte Multilayers via Counterion Exchange and in situ Reduction. *Langmuir* **2009**, *25*, 12355−12360.
(38) Peyratout, C. S.; Dähne, L. Tailor-made Polyelectrolyte Microcapsules: From Multilayers to Smart Containers. *Angew. Chem., Int. Ed.* **2004**, *43*, 3762−3783.
(39) Sides, P. J.; Newman, J.; Hoggard, J. D.; Prieve, D. C. Calculation of the Streaming Potential near a Rotating Disk. *Langmuir* **2006**, *22*, 9765−9769.
(40) Sides, P. J.; Hoggard, J. D. Measurement of the Zeta Potential of Planar Solid Surfaces by Means of a Rotating Disk. *Langmuir* **2004**, *20*, 11493−11498.
(41) Ferriz-Mañas, M.; Schlenoff, J. B. Zeta Potential of Polyelectrolyte Multilayers Using the Spinning Disk Method. *Langmuir* **2014**, *30*, 8776−8783.
(42) Haynes, W. M. *CRC Handbook of Chemistry and Physics*; CRC Press: Boca Raton, FL, 2014.
(43) Jaber, J. A.; Schlenoff, J. B. Mechanical Properties of Reversibly Cross-linked Ultrathin Polyelectrolyte Complexes. *J. Am. Chem. Soc.* **2006**, *128*, 2940−2947.
(44) Dautzenberg, H. Polyelectrolyte Complex Formation in Highly Aggregating Systems. 1. Effect of Salt: Polyelectrolyte Complex Formation in the Presence of NaCl. *Macromolecules* **1997**, *30*, 7810−7815.
(45) Jomaa, H. W.; Schlenoff, J. B. Salt-induced Polyelectrolyte Interdiffusion in Multilayered Films: A Neutron Reflectivity Study. *Macromolecules* **2005**, *38*, 8473−8480.
(46) Guzmán, E.; Ritacco, H.; Ortega, F.; Rubio, R. G. Evidence of the Influence of Adsorption Kinetics on the Internal Reorganization of Polyelectrolyte Multilayers. *Colloids Surf., A* **2011**, *384*, 274−281.
(47) Shamoun, R. F.; Hariri, H. H.; Ghostine, R. A.; Schlenoff, J. B. Thermal Transformations in Extruded Saloplastic Polyelectrolyte Complexes. *Macromolecules* **2012**, *45*, 9759−9767.
(48) Ghostine, R. A.; Jisr, R. M.; Lehaf, A.; Schlenoff, J. B. Roughness and Salt Annealing in a Polyelectrolyte Multilayer. *Langmuir* **2013**, *29*, 11742−11750.
(49) Zan, X. J.; Peng, B.; Hoagland, D. A.; Su, Z. H. Polyelectrolyte Uptake by PEMs: Impact of Salt Concentration. *Polym. Chem.* **2011**, *2*, 2581−2589.
(50) Han, L.; Mao, Z.; Wuliyasu, H.; Wu, J.; Gong, X.; Yang, Y.; Gao, C. Modulating the Structure and Properties of Poly(sodium 4-styrenesulfonate)/Poly(diallyldimethylammonium chloride) Multilayers with Concentrated Salt Solutions. *Langmuir* **2011**, *28*, 193−199.
(51) Dautzenberg, H.; Hartmann, J.; Grunewald, S.; Brand, F. Stoichiometry and Structure of Polyelectrolyte Complex Particles in Diluted Solutions. *Ber. Bunsen-Ges. Phys. Chem.* **1996**, *100*, 1024−1032.
(52) Sides, P. J.; Prieve, D. C. Surface Conductivity and the Streaming Potential near a Rotating Disk-Shaped Sample. *Langmuir* **2013**, *29*, 13427−13432.
(53) Hoggard, J. D.; Sides, P. J.; Prieve, D. C. Measurement of the Streaming Potential and Streaming Current near a Rotating Disk to Determine Its Zeta Potential. *Langmuir* **2005**, *21*, 7433−7438.
(54) In *Multilayer Thin films: Sequential Assembly of Nanocomposite Materials*, 2nd ed.; Decher, G., Schlenoff, J. B., Eds.; Wiley-VCH: Weinheim, 2012; p 2 v. (xxxiv, 1088 p.).

DOI: 10.1021/la504910y
Langmuir 2015, 31, 5787−5795

(55) Elbert, D. L.; Herbert, C. B.; Hubbell, J. A. Thin Polymer Layers Formed by Polyelectrolyte Multilayer Techniques on Biological Surfaces. *Langmuir* **1999**, *15*, 5355−5362.
(56) Lavalle, P.; Picart, C.; Mutterer, J.; Gergely, C.; Reiss, H.; Voegel, J. C.; Senger, B.; Schaaf, P. Modeling the Buildup of Polyelectrolyte Multilayer Films Having Exponential Growth. *J. Phys. Chem. B* **2004**, *108*, 635−648.
(57) Lehaf, A. M.; Hariri, H. H.; Schlenoff, J. B. Homogeneity, Modulus, and Viscoelasticity of Polyelectrolyte Multilayers by Nanoindentation: Refining the Buildup Mechanism. *Langmuir* **2012**, *28*, 6348−6355.
(58) Dubas, S. T.; Schlenoff, J. B. Swelling and Smoothing of Polyelectrolyte Multilayers by Salt. *Langmuir* **2001**, *17*, 7725−7727.
(59) Tanaka, T.; Sun, S. T.; Hirokawa, Y.; Katayama, S.; Kucera, J.; Hirose, Y.; Amiya, T. Mechanical Instability of Gels at the Phase-Transition. *Nature* **1987**, *325*, 796−798.
(60) Cerda, E.; Mahadevan, L. Geometry and Physics of Wrinkling. *Phys. Rev. Lett.* **2003**, *90*.

DOI: 10.1021/la504910y
Langmuir 2015, 31, 5787−5795